Non-Invasive In Vivo Assessment of Cardiac Metabolism in the Healthy and Diabetic Human Heart Using Hyperpolarized 13C MRI

Rider, O., Apps, A., Miller, J., Lau, J., Lewis, A., Peterzan, M., Dodd, M., Lau, A., Trumper, C., Gallagher, F., Grist, J., Brindle, K., Neubauer, S. & Tyler, D. J.

Non-Invasive In Vivo Assessment of Cardiac Metabolism in the Healthy and Diabetic Human Heart Using Hyperpolarized ^{13}C MRI

Oliver J Rider[1*], Andrew Apps[1*], Jack JJJ Miller[1,2,3], Justin YC Lau[1,2], Andrew JM Lewis[1], Mark A Peterzan[1], Michael S Dodd[4], Angus Z Lau[5], Claire Trumper[1], Ferdia A Gallagher[6], James T Grist[6], Kevin M Brindle[7], Stefan Neubauer[1†], Damian J Tyler[1,2†]

[1]Oxford Centre for Clinical Magnetic Resonance Research, Radcliffe Department of Medicine, University of Oxford, UK; [2]Department of Physiology, Anatomy and Genetics, University of Oxford, UK; [3]Department of Physics, University of Oxford, UK; [4]School of Life Sciences, Coventry University, UK; [5]Sunnybrook Research Institute, Toronto, Canada; [6]Department of Radiology, University of Cambridge, UK, and; [7]Cancer Research UK Cambridge Institute, University of Cambridge, UK.

*,† Authors contributed equally to this work

Running title: Hyperpolarized ^{13}C MRI in the Diabetic Human Heart

Address correspondence to:
Dr. Damian Tyler
Oxford Centre for Clinical Magnetic Resonance Research (OCMR)
Division of Cardiovascular Medicine, Radcliffe Department of Medicine
University of Oxford
Oxford, OX3 9DU
United Kingdom
damian.tyler@dpag.ox.ac.uk

ABSTRACT

**Rationale**: The recent development of hyperpolarized ^{13}C Magnetic Resonance Spectroscopy (MRS) has made it possible to measure cellular metabolism *in vivo*, in real time.
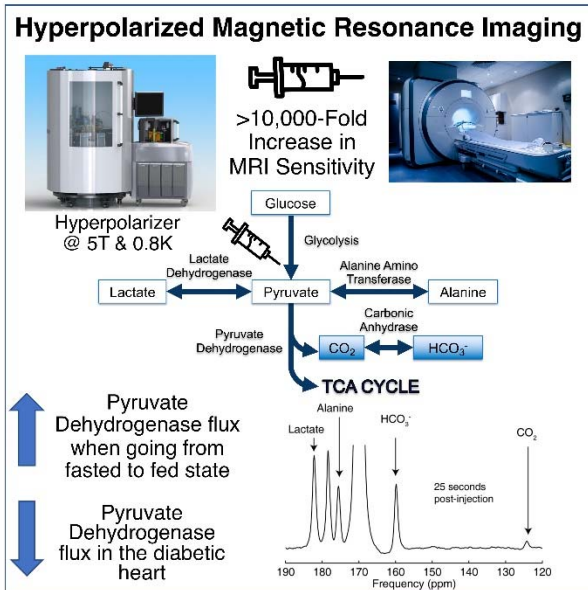
**Objective**: By comparing participants with and without type 2 diabetes (T2DM), we report the first case-control study to use this technique to record changes in cardiac metabolism in the healthy and diseased human heart.

**Methods and Results**: Thirteen people with type 2 diabetes (HbA1c 6.9±1.0%) and 12 age-matched healthy controls underwent assessment of cardiac systolic and diastolic function, myocardial energetics (^{31}P-MRS) and lipid content (^1H-MRS) in the fasted state. In a subset (5 T2DM, 5 control), hyperpolarized [1-^{13}C]pyruvate MR spectra were also acquired and in five of these participants (3 T2DM, 2 controls), this was successfully repeated 45 minutes after a 75g oral glucose challenge. Downstream metabolism of [1-^{13}C]pyruvate via pyruvate dehydrogenase (PDH, [^{13}C]bicarbonate), lactate dehydrogenase ([1-^{13}C]lactate) and alanine transaminase ([1-^{13}C]alanine) was assessed. Metabolic flux through cardiac PDH was significantly reduced in the people with type 2 diabetes (Fasted:0.0084±0.0067[Control] vs. 0.0016±0.0014[T2DM], Fed:0.0184±0.0109 vs. 0.0053±0.0041, p=.013). In addition, a significant increase in metabolic flux through PDH was observed after the oral glucose challenge (p<.001). As is characteristic of diabetes, impaired myocardial energetics, myocardial lipid content and diastolic function were also demonstrated in the wider study cohort.

**Conclusions**: This work represents the first demonstration of the ability of hyperpolarized ^{13}C MRS to non-invasively assess physiological and pathological changes in cardiac metabolism in the human heart. In doing so, we highlight the potential of the technique to detect and quantify metabolic alterations in the setting of cardiovascular disease.

Keywords:
Hyperpolarized magnetic resonance spectroscopy, diabetes mellitus, metabolism, pyruvate dehydrogenase, magnetic resonance imaging, diabetic cardiomyopathy.

Nonstandard Abbreviations and Acronyms:

ANOVA   Analysis of Variance
ATP   Adenosine Triphosphate
BMI   Body Mass Index
CMR   Cardiac Magnetic Resonance
DNP   Dynamic Nuclear Polarization
ECG   Electrocardiogram
EPA   Electron Paramagnetic Agent
FFA   Free Fatty Acids
HbA1c   Glycated Haemoglobin
HOMA-IR   Homeostatic Model Assessment of Insulin Resistance
LDH   Lactate Dehydrogenase
LV   Left Ventricular
LVEDV   Left Ventricular End Diastolic Volume
LVEF   Left Ventricular Ejection Fraction
MR   Magnetic Resonance
MRI   Magnetic Resonance Imaging
MRS   Magnetic Resonance Spectroscopy
PCr   Phosphocreatine
PDH   Pyruvate Dehydrogenase
PET   Positron Emission Tomography
RV   Right Ventricular
RVEDV   Right Ventricular End Diastolic Volume
RVEF   Right Ventricular Ejection Fraction
SNR   Signal-to-Noise Ratio
T2DM   Type 2 Diabetes Mellitus

INTRODUCTION.

Type 2 diabetes (T2DM), even in the absence of coronary artery disease and hypertension, is associated with a 2-5 fold increased risk of heart failure through the development of diabetic cardiomyopathy[1]. With the rapid global increase in the prevalence of obesity, and with it T2DM, it is very likely that there will be a similar increase in the prevalence of diabetic cardiomyopathy. As a result, there is a pressing need to improve our understanding of the mechanisms by which diabetes can cause heart failure and to develop non-invasive readouts of the mechanisms which underpin this process.

Several mechanisms have been implicated in the pathogenesis of diabetic cardiomyopathy with changes in myocardial structure, calcium signalling, and metabolism all described in animal models[2]. As the heart requires a vast amount of ATP to maintain contractile function, it is not surprising that there are functional consequences if metabolism is altered, and in T2DM, metabolic alteration is inherent to the underlying disease process. Although diabetes is characterized by an apparent abundance of substrate with increased circulating levels of both free fatty acids (FFA) and glucose, the diabetic myocardium utilizes almost exclusively FFA for the generation of ATP, and its metabolic flexibility is dramatically reduced[3]. This arises due to the combination of reduced glucose uptake[4] and increased fatty acid oxidation[5], which mediates an inhibition of pyruvate dehydrogenase (PDH) as described by the Randle cycle[6], resulting in a reduced efficiency of ATP production.

As both systole and diastole are ATP consuming processes, this leads to a proposed mechanism whereby reduced glucose oxidation acts, via impaired ATP production, to contribute to the development of

diabetic cardiomyopathy, with PDH being the central control point. In line with this, we have recently shown that by pharmacologically increasing PDH flux, and therefore rebalancing glucose utilization, it is possible to reverse the diastolic impairment observable in a rodent model of T2DM[7]. This highlights the importance of PDH in this process as a potential therapeutic target.

Mechanistic insights into diabetic cardiomyopathy to date have, in general, been gained either in animal models, due to the need for invasive procedures or destructive methods which are not feasible in humans, or using positron emission tomography (PET) and magnetic resonance spectroscopy (MRS). PET studies have revealed reductions in glucose uptake[8] and increases in fatty acid oxidation[9] whilst MRS studies have shown elevated myocardial triglyceride content[10] and impaired myocardial energetics[11], confirming to a large extent the findings in animal studies. However, gaining a window on important changes at the level of PDH has not been possible without invasive biopsies, making this impractical to assess as a routine biomarker.

One potential solution to this is ^{13}C MRS. This technique allows a direct evaluation of the activity of PDH by measuring the conversion of [1-^{13}C]pyruvate into [^{13}C]bicarbonate (H^{13}CO$_3^-$). However, although this is scientifically attractive, conventional ^{13}C MRS suffers from an inherently low sensitivity and low signal to noise ratio, making scan times very long and routine acquisition unfeasible at clinical field strengths. This low sensitivity can be overcome using the recent development of hyperpolarized MR technology, which can amplify the ^{13}C MRS signal by over 10,000-fold[12]. Using hyperpolarized [1-^{13}C]pyruvate, physiological changes in PDH flux have been demonstrated in animal models of feeding and fasting[13–15]. In addition, changes in cardiac substrate selection in a variety of pathological situations have been observed[16–18], particularly in diabetes[7,14,19,20].

The human applications of this technique are in their infancy, with an initial clinical demonstration in a study of patients with prostate cancer[21], and two smaller feasibility studies, one in the healthy heart[22] and another in the healthy brain[23]. Despite its potential, the assessment of either physiological or pathological changes in metabolic flux using hyperpolarized MRS have not yet been undertaken in the human heart.

As such, the primary aim of the work presented here was to provide the first non-invasive *in vivo* demonstration that physiological and pathological changes in PDH flux can be detected in the human heart using hyperpolarized [1-^{13}C]pyruvate MRS. By also assessing other hallmarks of diabetic heart disease, namely impaired energetics (^{31}P-MRS), myocardial steatosis (^{1}H-MRS), and diastolic impairment (echocardiography), we further aimed to determine the additional information that the hyperpolarized [1-^{13}C]pyruvate technique can provide in the detection of pathological changes in the diabetic heart.

METHODS

The data that support the findings of this study are available from the corresponding author upon reasonable request.

Study cohort and study visit.
This research was approved by the National Research Ethics Committee service (13/SW/0108) and conducted in accordance with the declaration of Helsinki and the Caldicott principles. All data collection was undertaken at the Oxford Centre for Clinical Magnetic Resonance at the John Radcliffe Hospital, Oxford, UK between March 2016 and May 2019. Written informed consent was obtained from all those enrolled. Thirteen people with type 2 diabetes and 12 controls were recruited from local advertisements.

All participants were aged >18, participants with type 2 diabetes were included if they had a recent HbA1c between 6 and 9%, no change of oral medications during the previous 3 months and were not on insulin therapy. Subjects with type 2 diabetes who were taking the oral anti-hyperglycaemic drug, Metformin, were asked to refrain from taking their medication for 12 hours before the study to minimise any potential effect on cardiac redox state[24].

All study visits began at 7 am following an overnight fast lasting at least 9 hours. Diastolic function (echocardiography), systolic function (CMR), myocardial steatosis (^{1}H-MRS) and myocardial energetics (^{31}P-MRS) were all assessed in the fasted state. Additionally, hyperpolarized [1-^{13}C]pyruvate MRS was undertaken immediately before and 45 minutes after a standardized oral glucose tolerance test consisting of a 75g glucose dose (taken in under 5 minutes; Rapilose®, Galen Ltd, Craigavon, United Kingdom). All MR scanning was undertaken at 3T (Tim Trio MR system, Siemens Healthineers, Erlangen, Germany).

The outline of our study visit is shown in Figure 1 and additional methodological details are given in the online supplement.

Dynamic Nuclear Polarization and production of hyperpolarized [1-^{13}C]pyruvate.

As described in the online supplement, all starting materials were prepared in a Grade A sterile environment[23] before being loaded into a General Electric SpinLab system (GE Healthcare, Chicago, USA) for the process of Dynamic Nuclear Polarization[12]. Sufficient polarization levels were achieved after 2-3 hours, after which dissolution was undertaken to produce the final hyperpolarized [1-^{13}C]pyruvate solution for injection. Solutions were only released for human injection if the following criteria were met: pH 6.7-8.4, temperature 25.0-37.0°C, polarization $\geq$ 15%, [pyruvate] 220-280 mM, [EPA] $\leq$ 3.0 μM, appearance: clear, colourless solution with no visible particulate matter. Administration of the hyperpolarized pyruvate was undertaken through an 18G venous cannula sited in the left antecubital fossa at a dose of 0.4 ml/kg and at a rate of 5 ml per second.

Hyperpolarized MR spectroscopy and data processing.

Subjects were scanned supine and hyperpolarized ^{13}C MR spectra were acquired using a 2 channel transmit, 8 channel surface-receive array (Rapid Biomedical, Rimpar, Germany). Hyperpolarized data were acquired from a mid-ventricular 10 mm axial slice, beginning at the start of the injection, using a pulse-acquire spectroscopy sequence acquired ECG-gated to the R-wave with a single slice-selective excitation every heartbeat and run for four minutes after injection. Total integrated metabolite-to-pyruvate ratios, known to linearly correlate with first-order chemical kinetic rate constants, were calculated by summing the first 60 seconds worth of spectral data acquired following the initial appearance of the hyperpolarized pyruvate resonance in the acquired spectra[25]. Further details are provided in the online supplement.

Statistical analysis.

All data was analyzed with the operator blinded to the disease status and metabolic state of the dataset. Hyperpolarized datasets, quantified as described above, were analysed with the *lme4* and the *car* packages in R (v3.6.0, R Foundation for Statistical Computing, Vienna, Austria), with metabolic state and disease status considered as fixed effects, and subject ID considered as a random effect, and an ANOVA table computed. Data were subject to a Shapiro-Wilk normality test and one outlier corresponding to the [^{13}C]bicarbonate to [1-^{13}C]pyruvate ratio for an unpaired fasted subject with type 2 diabetes with a Z-score of 9.4, was identified (Grubb's test p = .003, suggesting that point was an outlier). Data derived from this participant were excluded from subsequent analysis. No evidence of heteroscedasticity was found in the acquired ^{13}C data (Levene's test, p=.301 for [^{13}C]bicarbonate to [1-^{13}C]pyruvate ratio, p=.635 for [1-^{13}C]lactate to [1-^{13}C]pyruvate ratio and p=.751 for [1-^{13}C]alanine to [1-^{13}C]pyruvate ratio). This fact may reflect the comparatively high signal-to-noise ratio of the acquired spectral data, as it is known that the distribution of metabolite ratios is approximately normally distributed in the high SNR regime[26].

Unless otherwise stated, all other analyses were performed in GraphPad Prism (GraphPad Software, San Diego, California, USA) via simple unpaired unequal-variance *t*-tests with the canonical p<.05 threshold for statistical significance. All statistical tests performed are reported in Tables 1 & 2 with the exact p-values quoted, statistical significance is highlighted by italicising any reported p-values below 0.05.

RESULTS

Baseline population characterisation.

Healthy controls (n=12) and people with type 2 diabetes (n=13) were recruited with no difference in age (controls – 50.3±11.4 years, people with type 2 diabetes – 55.2±5.8 years, p=.190) or sex (controls – 8 male / 4 female, people with type 2 diabetes – 11 male, 2 female). Participants with type 2 diabetes had significantly higher body mass index (BMI) than controls (22.6±3.0 vs. 29.7±6.8, p=.003), but baseline myocardial structural characteristics assessed by cine-MRI including left ventricular ejection fraction (60±4% vs. 57±6%, p=.228), indexed left ventricular end-diastolic volume (82±12 ml/m^2 vs. 79±15 ml/m^2, p=.577) and myocardial mass index (64±10 g/m^2 vs. 62±11 g/m^2, p=.658), were not different between groups (Table 1). Participants with type 2 diabetes were confirmed to be more insulin resistant than the controls (HOMA-IR 1.3±0.8 vs. 4.3±2.5, p=.005), with higher fasting blood sugar. Five controls and five people with type 2 diabetes from within this cohort then went on to have fasting [1-^{13}C]pyruvate hyperpolarized MRS, with five (two control, three T2DM) receiving successful repeat [1-^{13}C]pyruvate hyperpolarized MRS 45 minutes after glucose ingestion. Again, this smaller hyperpolarized MRS group was well matched for age and myocardial structural characteristics (Table 1). Example data acquired from our study population are shown in Figure 2, demonstrating the breadth of metabolic and structural parameters acquired in a single scanning session.

Table 1: Characteristics of study population

Study Population	Control (n=12)	Diabetic (n=13)	p-Value
General			
Age (years)	50.3 ± 11.4	55.2 ± 5.8	.190
Weight (Kg)	68.0 ± 13.1	93.7 ± 17.7	*<.001*
BMI (Kg/m^2)	22.6 ± 3.0	29.7 ± 6.8	*.003*
HbA1c (%)	4.9 ± 0.3	6.9 ± 1.0	*<.001*
HOMA IR	1.3 ± 0.8	4.3 ± 2.5	*.005*
Fasting Glucose (mmol/l)	4.8 ± 0.7	7.9 ± 2.7	*.006*
Medication			
ACE-Inhibitor	0	6	-
Statin	0	9	-
Metformin	0	11	-
Sulfonylurea	0	5	-
Calcium Channel Blocker	0	2	-
Thiazide Diuretic	0	2	-
Asprin	0	2	-
Liraglutide	0	1	-
Sitagliptin	0	1	-
Echocardiography			
E/A	1.3 ± 0.4	1.0 ± 0.3	.127
E/e' (medial)	6.3 ± 2.0	8.1 ± 1.4	*.025*
E/e' (lateral)	5.1 ± 1.8	6.3 ± 1.8	.149
E/e' (mean)	5.7 ± 1.7	7.2 ± 1.4	*.040*
CMR			
LVEF (%)	60 ± 4	57 ± 6	.228
LVEDV Index (ml/m^2)	82 ± 12	79 ± 15	.577
LV Mass Index (g/m^2)	64 ± 10	62 ± 11	.658
RVEF (%)	54 ± 4	54 ± 6	.934
RVEDV Index (ml/m^2)	93 ± 8	84 ± 16	.095
Spectroscopy			
PCr/ATP	1.94 ± 0.21	1.71 ± 0.30	*.042*
Myocardial Lipid Content (% of water)	1.59 ± 0.88	3.05 ± 1.96	*.026*
^{13}C MRS Only Group	**Control (n=5)**	**Diabetic (n=5)**	
Age (years)	49.2 ± 13.1	52 ± 5.2	.668
Weight (Kg)	72.1 ± 7.4	99.2 ± 13.9	*.005*
BMI (Kg/m^2)	22.6 ± 1.7	31.1 ± 6.1	*.017*
E/e' (mean)	4.7 ± 1.1	6.6 ± 1.2	*.030*
PCr/ATP	2.03 ± 0.15	1.75 ± 0.35	.138
Myocardial Lipid Content (% of water)	1.29 ± 0.63	3.40 ± 2.26	.079

Injected hyperpolarized [1-^{13}C]pyruvate solution product specifications.

Hyperpolarized [1-^{13}C]pyruvate solution injections were well tolerated by all subjects with no side effects reported. Ten participants (five controls, five T2DM) received a total of 15 injections meeting the release criteria. The quality of these were highly standardized; mean (±SD) pyruvate concentration was 239±8 mM, residual EPA 1.1±0.7 µM, pH 7.7±0.4, temperature 34±1°C and polarization 34±13%. The mean polarization time was 150±30 minutes and dissolution to injection times were all less than 90 seconds.

Hyperpolarized ^{13}C magnetic resonance spectroscopy.

Acquired hyperpolarized spectra were of high quality with peaks corresponding to [^{13}C]bicarbonate, ^{13}CO$_2$, [1-^{13}C]lactate and [1-^{13}C]alanine (the downstream metabolites of [1-^{13}C]pyruvate), clearly visible and appearing 2-3 seconds after the ventricular [1-^{13}C]pyruvate resonance. Example fed and fasted summed spectra from both a control and subject with type 2 diabetes are shown in Figure 3, with typical time courses of substrate and metabolite signal intensities for a control and a subject with type 2 diabetes also shown. A summary of time-integrated metabolite to substrate ratios derived from the *in vivo* hyperpolarized ^{13}C MRS data can be found in Table 2.

Table 2: Time-integrated metabolite to substrate ratios derived from hyperpolarized ^{13}C MR data

	Control (n=5)		Diabetic (n=5)		p-Value		
	Fasted (n=5)	Fed (n=2)	Fasted (n=5)	Fed (n=3)	Metabolic state	Diseased state	Interaction
Bic/Pyr (x10^{-2})	0.84 ± 0.67	1.84 ± 1.09	0.16 ± 0.14	0.53 ± 0.41	*<.001*	*.013*	*.040*
Lac/Pyr (x10^{-2})	5.16 ± 1.52	5.94 ± 2.01	8.51 ± 1.38	10.53 ± 1.38	.072	*<.001*	.455
Bic / Lac	0.15 ± 0.10	0.30 ± 0.08	0.02 ± 0.02	0.05 ± 0.03	*<.001*	*<.001*	*.008*
Ala/Pyr (x10^{-2})	3.17 ± 1.11	3.70 ± 2.03	3.82 ± 1.05	4.74 ± 0.66	.077	.257	.690

The [^{13}C]bicarbonate to [1-^{13}C]pyruvate ratio, shown previously to linearly correlate with enzymatic flux through PDH, was significantly reduced by diabetes (5.3-fold reduction when fasted and 3.5-fold reduction when fed, p=.013). Conversely, the [1-^{13}C]lactate to [1-^{13}C]pyruvate ratio, reflecting exchange through LDH, was increased by diabetes (1.6-fold increase when fasted and 1.8-fold increase when fed, p<.001). As a marker of the balance between glycolytic and oxidative carbohydrate metabolism[27], the ratio of [^{13}C]bicarbonate and [1-^{13}C]lactate signals showed a significant reduction in relative carbohydrate oxidation in the subjects with type 2 diabetes (7.5-fold reduction when fasted and 6-fold reduction when fed, p<.001). Transamination of [1-^{13}C]pyruvate to [1-^{13}C]alanine was not different between subjects with type 2 diabetes and controls (p=.257). Comparisons of enzymatic flux data as assessed by hyperpolarized MRS are summarized in Figure 4.

Hyperpolarized MRS also successfully demonstrated Randle cycle associated increases in PDH flux after feeding with flux significantly increased 45 minutes after the oral administration of 75 g of glucose (p<.001). Importantly, this increase was discernible not only in controls (2.2-fold increase), but also in the subjects with type 2 diabetes (3.3-fold increase), in spite of the impaired basal PDH flux we have demonstrated in this condition. There were no statistically significant differences in LDH flux (p=.072) or the rate of pyruvate transamination (p=.077) between the fasted and fed states.

[31]P and ^{1}H magnetic resonance spectroscopy.

As expected, within the wider study population, diabetes significantly impaired cardiac diastolic function (mean E/e' 5.7±1.7 vs. 7.2±1.4, p=.040), myocardial energetics (PCr/ATP 1.94±0.21 vs. 1.71±0.30, p=.042) and increased myocardial triglyceride content (1.59±0.88 vs. 3.05±1.96, p=.026). The effect sizes for these differences (E/e'=0.963, PCr/ATP=0.888, myocardial triglyceride content=0.961, G*Power 3.1) were all lower than the effect sizes calculated for the differences observed between the fasted controls and the subjects with type 2 diabetes from the ^{13}C enzymatic flux data reported above (bicarbonate/pyruvate = 1.405, lactate/pyruvate = 2.308, bicarbonate/lactate = 1.803). This means that, when comparing two groups with a simple Students t-test, to observe the differences seen here at a p-value of 0.05 with a power of 90% would require group sizes of 24, 28 and 24 for E/e', PCr/ATP and myocardial triglyceride content respectively versus group sizes of 12, 6 and 8 for bicarbonate/pyruvate, lactate/pyruvate and bicarbonate/lactate respectively (G*Power 3.1).

Weak correlations were observed between the PCr/ATP ratio and the metabolic parameters assessed by hyperpolarized MRS (i.e. positive correlations between PCr/ATP and the bicarbonate/pyruvate, alanine/pyruvate and bicarbonate/lactate ratios and a negative correlation between PCr/ATP and the lactate/pyruvate ratio, but these failed to reach statistical significance, Supplementary Figure I).

DISCUSSION

In the setting of the rapid global increase in T2DM and its relationship with heart failure, increasing our understanding of the metabolic changes that occur in diabetes is becoming increasingly important. Using a hyperpolarized [1-^{13}C]pyruvate tracer, we have shown that, following glucose ingestion, the myocardium increases pyruvate oxidation through PDH (PDH Flux), in line with the metabolic alterations proposed by the Randle cycle[6]. In addition, we have also shown in patients with type 2 diabetes and diastolic dysfunction that PDH flux is reduced, similarly to alterations seen in animal models[7,20]. This, therefore, represents the first non-invasive demonstration of physiological and pathological changes in PDH flux in the human heart using hyperpolarized MRS. Furthermore, we have used ^{31}P and ^{1}H spectroscopy to confirm that, in the presence of reduced PDH flux, the diabetic myocardium has reduced myocardial energetics (PCr/ATP ratio) and increased myocardial triglyceride content. This is the first human study to use the multi-nuclear combination of ^{1}H, ^{31}P and ^{13}C MR spectroscopy to interrogate myocardial metabolism and confirms the potential of hyperpolarized MRS for translation to the clinical quantification of metabolic alterations in cardiac pathology.

Pyruvate dehydrogenase flux.

Our demonstration that the fasted heart increases PDH flux after an oral glucose challenge is consistent with the Randle cycle and confirms previous hyperpolarized [1-^{13}C]pyruvate experiments in mice[13], rats[14] and pigs[15]. Whilst this is an expected result, it is the first demonstration in humans that hyperpolarized [1-^{13}C]pyruvate MR can detect physiological changes in myocardial metabolism, an important milestone in its clinical translation.

As the post-glucose scan was undertaken ~one hour after the initial fasted scan, there is the possibility that the injected pyruvate dose from the first scan may also have played a part in the increased PDH flux observed. However, it seems unlikely that the ~1 g dose of pyruvate given would have had a significant impact on top of the 75g of glucose provided. The variation in PDH flux observed between the fed and fasted states also illustrates that, when considering myocardial metabolic readouts, there is a need to standardize (or at least establish) the prevailing metabolic conditions under which they are made. To

date, animal models have used glucose loading prior to hyperpolarized studies to maximize baseline PDH flux, increasing the power of studies aiming to detect pathological changes.

In contrast to the normal heart, which has metabolic flexibility, the diabetic heart becomes almost exclusively reliant upon fatty acids as its main catabolic substrate. This overreliance on fat metabolism is likely underpinned by an impaired ability to uptake glucose and oxidize the resulting pyruvate through PDH. Indeed, animal models of diabetes have shown PDH inhibition both *ex vivo*[28] and *in vivo*[14]. In line with this, we have shown here in people with type 2 diabetes, that myocardial PDH flux is reduced compared to the normal healthy heart. Minimal discernible flux through PDH was observed in the fasted diabetic state, with only a small increase demonstrated after glucose loading, however, our findings show that hyperpolarized [1-13C]pyruvate studies aimed at measuring alterations in PDH flux in patients with type 2 diabetes are indeed feasible.

Linking altered substrate metabolism to altered function.

As diastole is more susceptible to ATP shortage than systole, alterations in substrate selection may act via reduced efficiency of ATP production initially as diastolic dysfunction, which is an almost universal finding in type 2 diabetes[29,30]. In line with this, we have shown here that the diabetic myocardium has reduced pyruvate oxidation (reflective of reduced glucose utilization), increased triglyceride deposition (suggestive of excess fatty acid uptake), reduced myocardial energetics (with reduced PCr/ATP) and diastolic dysfunction. As the diabetic phenotype in this study was not advanced or severe (we excluded subjects requiring exogenous insulin; average HbA1c was 6.9%), this highlights the metabolic inflexibility of the cardiomyocyte in the setting of lower grades of insulin resistance, and also the ability of hyperpolarized MR to detect early changes in myocardial metabolism in diabetes.

Lactate dehydrogenase flux.

Incorporation of the 13C label into [1-13C]lactate in our acquired spectra was significantly higher in subjects with type 2 diabetes in both fasted and fed states suggesting raised LDH flux in this group. Although it could be assumed that given [1-13C]pyruvate flux through PDH was lower, that LDH flux, and therefore the lactate pool size[31], would be reciprocally increased, this interpretation may be too simplistic. Other factors should be considered, for example it has previously been demonstrated that the antihyperglycemic agent, Metformin, has an effect on cardiac redox state that elevates the observed lactate signal[24]. To minimise this effect, the subjects with type 2 diabetes studied were asked to refrain from taking their Metformin on the day of the study. However, we cannot exclude the possibility that a chronic effect of their Metformin treatment may have contributed to the elevated lactate signal observed.

In addition, the myocardial [1-13C]lactate signal following injection of [1-13C]pyruvate has proven much more diffuse in hyperpolarized short axis images of the both the human[22] and pig heart[32] with a large contribution from the blood pool. Therefore, [1-13C]lactate generated in, and effluxed from, the liver may also be contaminating the cardiac readouts[33]. As such, we must be cautious in interpreting the exact derivation of the increased lactate signal from non-localized spectra. With metabolite imaging now possible in the human heart[22], this will aid in the localization of the lactate signal and discern whether or not its origin is myocardial.

Alanine aminotransferase flux.

In *ex vivo* models, the rate of pyruvate transamination has been shown to increase proportionally as pyruvate perfusate concentration increases. Labelled alanine is thus a direct measure of the intra-cellular availability of labelled pyruvate and the alanine signal has therefore been suggested as an alternative normalization standard (as opposed to the pyruvate signal)[34]. Relative stability of [1-13C]alanine signals

in our study, and lack of difference between groups, suggests cellular bioavailability of administered [1-^{13}C]pyruvate was uniform, and not a potential confounder of the variation of enzymatic fluxes seen.

Wider translation to clinical practice.

The technology of dissolution DNP is still in its infancy. The first demonstration of clinical translation was published in 2013 using a prototype polarizer located inside a cleanroom to prepare sterile injections for prostate cancer patients[21]. The SpinLab is the clinical grade second generation of polarizer suitable for preparing sterile injections outside of a controlled pharmaceutical facility, and currently 10 sites worldwide are injecting hyperpolarized compounds in early-phase clinical trials. Using this clinical system, we have demonstrated the first step in the clinical translation into cardiovascular disease characterization through the observation of metabolic flux changes in the normal and the diabetic human heart. While technically challenging, leading in part to our work being performed on a comparatively small number of subjects, the large effect size of metabolic dysregulation in disease is such that significant differences in myocardial metabolism, known extensively to exist from several decades of previous animal experimentation, as well as the effects of novel therapies, can be conclusively demonstrated in the human heart. Future studies should build on this proof-of-principle to explore the impact of other cardiovascular diseases, as well as the role that possible confounding factors (such as age, sex, medication use) might have on cardiac metabolism.

As hyperpolarized ^{13}C-imaging allows the *in vivo* visualization of cardiac metabolism, it has major advantages over current non-invasive imaging techniques. Hyperpolarized scans are fast (<2 mins), have no ionizing radiation, and, due to the ability to simultaneously acquire standard MRI acquisitions, have the potential to directly assess perfusion, ischemia, viability, and altered substrate selection in one imaging session. However, the technique does have some limitations. Firstly, the rapid decay of the hyperpolarized signal (i.e. the T_1 of hyperpolarized [1-^{13}C]pyruvate in solution has been measured to be 67.3 ± 2.5 s at 3T[35]) leads to the requirement to undertake the hyperpolarization process adjacent to the MRI system and to inject the hyperpolarized tracer immediately after production. Whilst this offers some technical challenges, the work reported here and by others[21–23] demonstrates that these challenges, as with short-lived PET tracers, can be overcome.

Secondly, in contrast to PET systems, which are capable of measuring picomolar amounts of radiolabelled molecules, hyperpolarized pyruvate scans require injection of the tracer at millimolar concentrations. It has previously been suggested that this "supra-physiological" dose of pyruvate may impact the metabolic processes that are being assessed. However, pre-clinical work in animals has shown that similar doses (~320 mol/kg in previous rat studies versus the ~140 mol/kg used in this work) leads to maximum plasma pyruvate concentrations of approximately 250 μM, equivalent to physiological pyruvate concentrations reached during exercise or with dietary interventions[34]. In addition, pre-clinical studies have demonstrated tight correlations between *in vivo* hyperpolarized MRS measurements of PDH flux and *ex vivo* measurements of PDH enzyme activity[34].

Whilst the work described here was undertaken at 3T, there are advantages and disadvantages to undertaking hyperpolarized experiments at different field strengths. Higher field strengths provide increased spectral separation between different metabolites and the subsequent benefits in quantification and selection of different metabolites for spectral imaging that this brings. Alternatively, the longitudinal relaxation times of hyperpolarized agents are generally longer at lower field strengths[35] and there is improved B_0 homogeneity which will improve spectral linewidths. As such, 3T seems a reasonable compromise between these competing factors for such initial proof-of-concept studies.

In conclusion, this study provides the first demonstration of the ability of hyperpolarized pyruvate to non-invasively assess physiological and pathological changes in pyruvate dehydrogenase flux in the human heart. In doing so, we highlight the potential of the technique to assess metabolic alterations in a range of cardiovascular diseases.

DISCLOSURES.

Dr Gallagher has received research support from GE Healthcare. Prof. Brindle holds patents in the field of hyperpolarized MRI relating to the use of imaging media comprising lactate and hyperpolarized [^{13}C]pyruvate, ^{13}C-MR imaging or spectroscopy of cell death, hyperpolarized lactate as a contrast agent for determination of LDH activity and imaging of ethanol metabolism. In addition, Prof. Brindle has research agreements with GE Healthcare which involve the use of hyperpolarized MRI technology. Prof Tyler holds a patent relating to the use of hyperpolarized [1-^{13}C]pyruvate for the assessment of PDH flux and has research agreements with GE Healthcare which involve the use of hyperpolarized MRI technology. No other authors have any conflicts of interest.

SUPPLEMENTAL MATERIALS

Expanded Materials & Methods
Supplemental Tables I - II
Supplemental Figure I
Major Resources Table
References: [10,23,36–47]

REFERENCES

[1] Adams KF, Schatzkin A, Harris TB, Kipnis V, Mouw T, Ballard-Barbash R, et al. Overweight, Obesity, and Mortality in a Large Prospective Cohort of Persons 50 to 71 Years Old. N Engl J Med 2006. doi:10.1056/nejmoa055643.

[2] Boudina S, Abel ED. Diabetic cardiomyopathy, causes and effects. Rev Endocr Metab Disord 2010. doi:10.1007/s11154-010-9131-7.

[3] Heather LC, Clarke K. Metabolism, hypoxia and the diabetic heart. J Mol Cell Cardiol 2011. doi:10.1016/j.yjmcc.2011.01.007.

[4] Randle PJ, Kerbey AL, Espinal J. Mechanisms decreasing glucose oxidation in diabetes and starvation: Role of lipid fuels and hormones. Diabetes Metab Rev 1988. doi:10.1002/dmr.5610040702.

[5] Wright JJ, Kim J, Buchanan J, Boudina S, Sena S, Bakirtzi K, et al. Mechanisms for increased myocardial fatty acid utilization following short-term high-fat feeding. Cardiovasc Res 2009. doi:10.1093/cvr/cvp017.

[6] Randle PJ, Garland PB, Hales CN, Newsholme EA. THE GLUCOSE FATTY-ACID CYCLE ITS ROLE IN INSULIN SENSITIVITY AND THE METABOLIC DISTURBANCES OF DIABETES MELLITUS. Lancet 1963. doi:10.1016/S0140-6736(63)91500-9.

[7] Page LML, Rider OJ, Lewis AJ, Ball V, Clarke K, Johansson E, et al. Increasing pyruvate dehydrogenase flux as a treatment for diabetic cardiomyopathy: A combined 13C hyperpolarized magnetic resonance and echocardiography study. Diabetes 2015. doi:10.2337/db14-1560.

[8] Peterson LR, Herrero P, Coggan AR, Kisrieva-Ware Z, Saeed I, Dence C, et al. Type 2 diabetes, obesity, and sex difference affect the fate of glucose in the human heart. Am J Physiol - Hear Circ Physiol 2015. doi:10.1152/ajpheart.00722.2014.

[9] Herrero P, Peterson LR, McGill JB, Matthew S, Lesniak D, Dence C, et al. Increased myocardial fatty acid metabolism in patients with type 1 diabetes mellitus. J Am Coll Cardiol 2006. doi:10.1016/j.jacc.2005.09.030.

[10] Levelt E, Rodgers CT, Clarke WT, Mahmod M, Ariga R, Francis JM, et al. Cardiac energetics, oxygenation, and perfusion during increased workload in patients with type 2 diabetes mellitus. Eur Heart J 2016. doi:10.1093/eurheartj/ehv442.

[11] Scheuermann-Freestone M, Madsen PL, Manners D, Blamire AM, Buckingham RE, Styles P, et al. Abnormal cardiac and skeletal muscle energy metabolism in patients with type 2 diabetes. Circulation 2003. doi:10.1161/01.CIR.0000072789.89096.10.

[12] Ardenkjaer-Larsen JH, Fridlund B, Gram A, Hansson G, Hansson L, Lerche MH, et al. Increase in signal-to-noise ratio of > 10,000 times in liquid-state NMR. Proc Natl Acad Sci U S A 2003;100:10158–10163. doi:10.1073/pnas.1733835100.

[13] Dodd MS, Ball V, Bray R, Ashrafian H, Watkins H, Clarke K, et al. In vivo mouse cardiac hyperpolarized magnetic resonance spectroscopy. J Cardiovasc Magn Reson 2013. doi:10.1186/1532-429X-15-19.

[14] Schroeder MA, Cochlin LE, Heather LC, Clarke K, Radda GK, Tyler DJ. In vivo assessment of pyruvate dehydrogenase flux in the heart using hyperpolarized carbon-13 magnetic resonance. Proc Natl Acad Sci 2008. doi:10.1073/pnas.0805953105.

[15] Tougaard RS, Szocska Hansen ES, Laustsen C, Nørlinger TS, Mikkelsen E, Lindhardt J, et al. Hyperpolarized [1- 13 C]pyruvate MRI can image the metabolic shift in cardiac metabolism between the fasted and fed state in a porcine model. Magn Reson Med 2019. doi:10.1002/mrm.27560.

[16] O h-Ici D, Wespi P, Busch J, Wissmann L, Krajewski M, Weiss K, et al. Hyperpolarized Metabolic MR Imaging of Acute Myocardial Changes and Recovery after Ischemia-Reperfusion in a Small-Animal Model. Radiology 2015. doi:10.1148/radiol.2015151332.

[17] Tougaard RS, Hansen ESS, Laustsen C, Lindhardt J, Schroeder M, Bøtker HE, et al. Acute hypertensive stress imaged by cardiac hyperpolarized [1- 13 C]pyruvate magnetic resonance. Magn

Reson Med 2018. doi:10.1002/mrm.27164.

[18]   Atherton HJ, Dodd MS, Heather LC, Schroeder MA, Griffin JL, Radda GK, et al. Role of pyruvate dehydrogenase inhibition in the development of hypertrophy in the hyperthyroid rat heart: A combined magnetic resonance imaging and hyperpolarized magnetic resonance spectroscopy study. Circulation 2011. doi:10.1161/CIRCULATIONAHA.110.011387.

[19]   Rohm M, Savic D, Ball V, Curtis MK, Bonham S, Fischer R, et al. Cardiac dysfunction and metabolic inflexibility in a mouse model of diabetes without dyslipidemia. Diabetes 2018. doi:10.2337/db17-1195.

[20]   Le Page LM, Ball DR, Ball V, Dodd MS, Miller JJ, Heather LC, et al. Simultaneous in vivo assessment of cardiac and hepatic metabolism in the diabetic rat using hyperpolarized MRS. NMR Biomed 2016. doi:10.1002/nbm.3656.

[21]   Nelson SJ, Kurhanewicz J, Vigneron DB, Larson PEZ, Harzstark AL, Ferrone M, et al. Metabolic imaging of patients with prostate cancer using hyperpolarized [1-13C]pyruvate. Sci Transl Med 2013. doi:10.1126/scitranslmed.3006070.

[22]   Cunningham CH, Lau JYC, Chen AP, Geraghty BJ, Perks WJ, Roifman I, et al. Hyperpolarized 13C Metabolic MRI of the Human Heart: Initial Experience. Circ Res 2016. doi:10.1161/CIRCRESAHA.116.309769.

[23]   Grist JT, McLean MA, Riemer F, Schulte RF, Deen SS, Zaccagna F, et al. Quantifying normal human brain metabolism using hyperpolarized [1– 13 C]pyruvate and magnetic resonance imaging. Neuroimage 2019. doi:10.1016/j.neuroimage.2019.01.027.

[24]   Lewis AJM, Miller JJJ, McCallum C, Rider OJ, Neubauer S, Heather LC, et al. Assessment of metformin-induced changes in cardiac and hepatic redox state using hyperpolarized [1-13C]pyruvate. Diabetes 2016. doi:10.2337/db16-0804.

[25]   Hill DK, Orton MR, Mariotti E, Boult JKR, Panek R, Jafar M, et al. Model Free Approach to Kinetic Analysis of Real-Time Hyperpolarized 13C Magnetic Resonance Spectroscopy Data. PLoS One 2013. doi:10.1371/journal.pone.0071996.

[26]   Miller JJ, Cochlin L, Clarke K, Tyler DJ. Weighted averaging in spectroscopic studies improves statistical power. Magn Reson Med 2017. doi:10.1002/mrm.26615.

[27]   Merritt ME, Harrison C, Storey C, Sherry a D, Malloy CR. Inhibition of carbohydrate oxidation during the first minute of reperfusion after brief ischemia: NMR detection of hyperpolarized 13CO2 and H13CO3-. Magn Reson Med 2008;60:1029–1036. doi:10.1002/mrm.21760.

[28]   Wieland O, Siess E, Schulze-Wethmar FH, von Funcke HG, Winton B. Active and inactive forms of pyruvate dehydrogenase in rat heart and kidney: effect of diabetes, fasting, and refeeding on pyruvate dehydrogenase interconversion. Arch Biochem Biophys 1971;143:593–601. doi:10.1016/0003-9861(71)90244-x.

[29]   Peterson LR, Waggoner AD, Schechtman KB, Meyer T, Gropler RJ, Barzilai B, et al. Alterations in left ventricular structure and function in young healthy obese women: Assessment by echocardiography and tissue Doppler imaging. J Am Coll Cardiol 2004. doi:10.1016/j.jacc.2003.10.062.

[30]   Otto ME, Belohlavek M, Khandheria B, Gilman G, Svatikova A, Somers V. Comparison of right and left ventricular function in obese and nonobese men. Am J Cardiol 2004. doi:10.1016/j.amjcard.2004.02.073.

[31]   Day SE, Kettunen MI, Gallagher F a, Hu D-E, Lerche M, Wolber J, et al. Detecting tumor response to treatment using hyperpolarized 13C magnetic resonance imaging and spectroscopy. Nat Med 2007;13:1382–1387. doi:10.1038/nm1650.

[32]   Lau AZ, Chen AP, Barry J, Graham JJ, Dominguez-Viqueira W, Ghugre NR, et al. Reproducibility study for free-breathing measurements of pyruvate metabolism using hyperpolarized 13C in the heart. Magn Reson Med 2013. doi:10.1002/mrm.24342.

[33]   Wespi P, Steinhauser J, Kwiatkowski G, Kozerke S. Overestimation of cardiac lactate production caused by liver metabolism of hyperpolarized [1- 13 C]pyruvate. Magn Reson Med 2018. doi:10.1002/mrm.27197.

[34] Atherton HJ, Schroeder MA, Dodd MS, Heather LC, Carter EE, Cochlin LE, et al. Validation of the in vivo assessment of pyruvate dehydrogenase activity using hyperpolarised 13C MRS. NMR Biomed 2011. doi:10.1002/nbm.1573.

[35] Wilson DM, Keshari KR, Larson PEZ, Chen AP, Hu S, Criekinge M Van, et al. Multi-compound polarization by DNP allows simultaneous assessment of multiple enzymatic activities in vivo. J Magn Reson 2010. doi:10.1016/j.jmr.2010.04.012.

[36] Nagueh SF, Appleton CP, Gillebert TC, Marino PN, Oh JK, Smiseth OA, et al. Recommendations for the evaluation of left ventricular diastolic function by echocardiography. Eur J Echocardiogr 2009. doi:10.1093/ejechocard/jep007.

[37] Hudsmith LE, Petersen SE, Francis JM, Robson MD, Neubauer S. Normal human left and right ventricular and left atrial dimensions using steady state free precession magnetic resonance imaging. J Cardiovasc Magn Reson 2005. doi:10.1080/10976640500295516.

[38] Rial B, Robson MD, Neubauer S, Schneider JE. Rapid quantification of myocardial lipid content in humans using single breath-hold 1H MRS at 3 Tesla. Magn Reson Med 2011. doi:10.1002/mrm.23011.

[39] Vanhamme L, Van Den Boogaart A, Van Huffel S. Improved Method for Accurate and Efficient Quantification of MRS Data with Use of Prior Knowledge. J Magn Reson 1997. doi:10.1006/jmre.1997.1244.

[40] Tyler DJ, Emmanuel Y, Cochlin LE, Hudsmith LE, Holloway CJ, Neubauer S, et al. Reproducibility of 31P cardiac magnetic resonance spectroscopy at 3 T. NMR Biomed 2009. doi:10.1002/nbm.1350.

[41] Purvis LAB, Clarke WT, Biasiolli L, Valkovič L, Robson MD, Rodgers CT. OXSA: An open-source magnetic resonance spectroscopy analysis toolbox in MATLAB. PLoS One 2017. doi:10.1371/journal.pone.0185356.

[42] Ardenkjaer-Larsen JH, Leach AM, Clarke N, Urbahn J, Anderson D, Skloss TW. Dynamic nuclear polarization polarizer for sterile use intent. NMR Biomed 2011. doi:10.1002/nbm.1682.

[43] Rodgers CT, Robson MD. Receive array magnetic resonance spectroscopy: Whitened singular value decomposition (WSVD) gives optimal bayesian solution. Magn Reson Med 2010. doi:10.1002/mrm.22230.

[44] Daniels CJ, Mclean MA, Schulte RF, Robb FJ, Gill AB, Mcglashan N, et al. A comparison of quantitative methods for clinical imaging with hyperpolarized 13C-pyruvate. NMR Biomed 2016. doi:10.1002/nbm.3468.

[45] Harrison XA, Donaldson L, Correa-Cano ME, Evans J, Fisher DN, Goodwin CED, et al. A brief introduction to mixed effects modelling and multi-model inference in ecology. PeerJ 2018. doi:10.7717/peerj.4794.

[46] Bates D, Mächler M, Bolker B, Walker S. Fitting Linear Mixed-Effects Models Using **lme4**. J Stat Softw 2015. doi:10.18637/jss.v067.i01.

[47] Tietjen GL, Moore RH. Some Grubbs-Type Statistics for the Detection of Several Outliers. Technometrics 1972. doi:10.1080/00401706.1972.10488948.

FIGURE LEGENDS

Figure 1: Outline of our typical study visit. The fasting stipulation in our study restricted our recruitment to what can be considered a fairly mild phenotype of diabetes – only those patients receiving oral medication. The total study visit was under three hours; however, each hyperpolarized MRS scan took only a few minutes, meaning its addition to the normal length of routine MR protocols would be insignificant.

Figure 2: Example data collected during our study from a recruited control (top row) and a subject with type 2 diabetes (bottom row). In characterizing our recruits both structurally (CMR / Echo) and metabolically (^{31}P MRS, ^{1}H MRS, hyperpolarized ^{13}C MRS), we collate the most comprehensive study of the diabetic cardiac phenotype to date.

Figure 3: Representative examples of hyperpolarized MR spectra from both a healthy control and a subject with type 2 diabetes in both the fasted and fed states, with ^{13}C containing downstream metabolites labelled. The [^{13}C]bicarbonate resonance is visibly reduced in the subject with type 2 diabetes with increases seen during feeding in both controls and subjects with type 2 diabetes. Time courses of the normalized signal amplitudes of downstream ^{13}C-labelled metabolic products of administered [1-^{13}C]pyruvate (shown in blue), in both a control and a subject with type 2 diabetes are also shown.

Figure 4: Plots of metabolic flux data for each metabolic product of administered [1-^{13}C]pyruvate. Flux through PDH (Bicarbonate, A) is reduced in the subjects with type 2 diabetes (p=.013), with increases seen during feeding (p<.001, E). Levels of [1-^{13}C]lactate were significantly higher in the hearts of people with type 2 diabetes (p<.001, B) with no change observed upon feeding (F). The ratio of bicarbonate and lactate was significantly lower in the subjects with type 2 diabetes (p<.001, C) and was elevated by feeding (p<.001, G). No significant differences in [1-^{13}C]alanine were seen across all injections (D,H). † p<.05 in subjects with type 2 diabetes vs. controls, * p<.05 in fasted subjects vs. fed, 'x' indicates the data point excluded as an outlier.
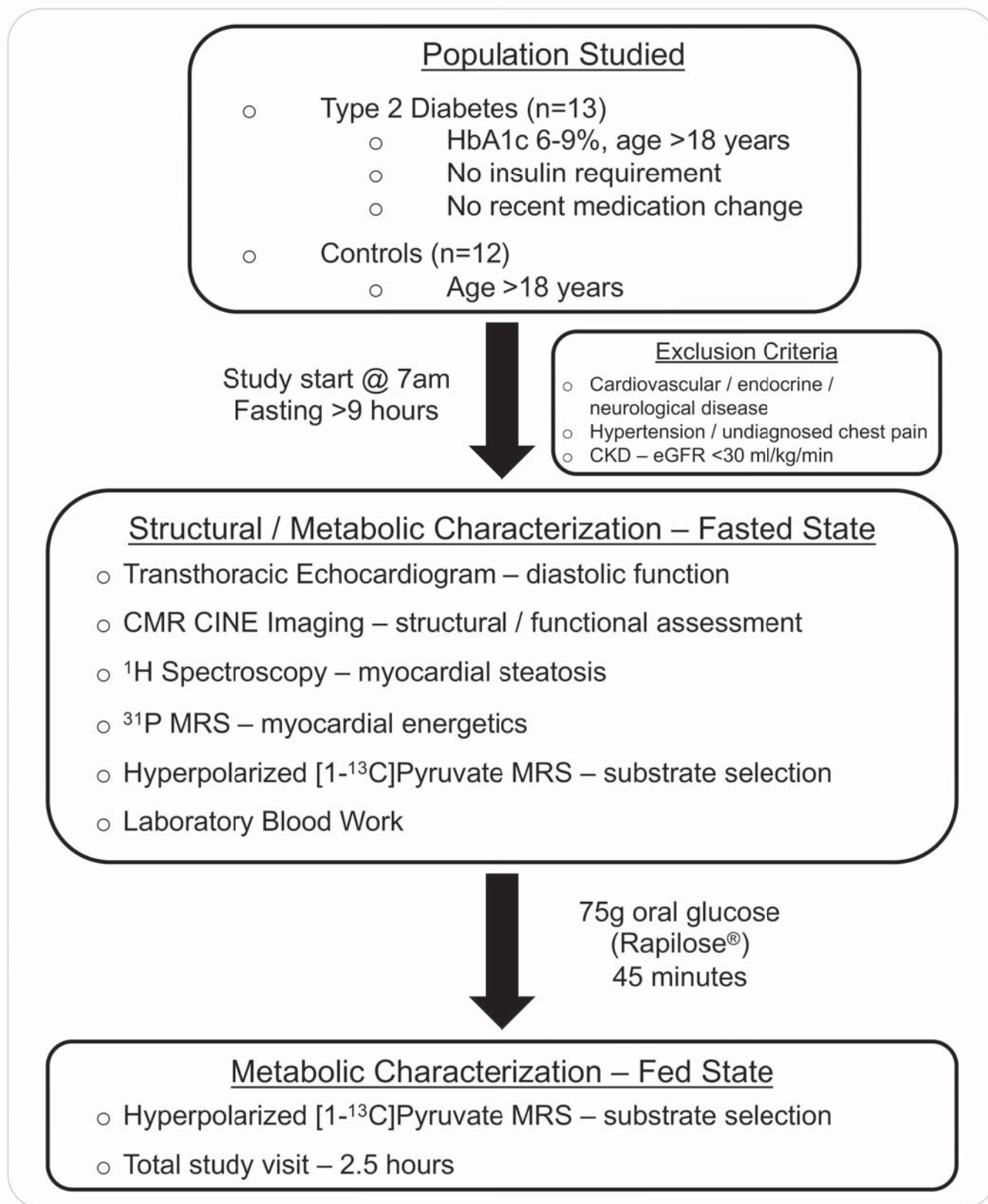
NOVELTY AND SIGNIFICANCE

What Is Known?

• The way the heart turns fuels (e.g. fats, glucose) into energy, called metabolism, is altered in many types of heart disease.

• However, we have very limited techniques available to allow us to measure metabolism in patients.

What New Information Does This Article Contribute?

• This article demonstrates the first use of a new technique, called hyperpolarized ^{13}C magnetic resonance imaging (MRI), for measuring changes in cardiac metabolism in healthy controls and people with diabetes.

• We show here that hyperpolarized ^{13}C MRI can detect increases in the metabolism of carbohydrates (e.g. glucose) when people go from being fasted to fed and also that carbohydrate metabolism is significantly reduced in the diabetic heart.

Alterations in cardiac metabolism are a hallmark of many cardiovascular diseases but current imaging techniques have a limited ability to study cardiac metabolism non-invasively. The emerging technique of hyperpolarized ^{13}C MRI offers >10,000-fold gains in the sensitivity of MRI for the assessment of cardiac metabolism. This work demonstrates the first step in the clinical translation of this exciting new technology into cardiovascular disease characterization through the observation of metabolic flux changes in the normal and the diabetic human heart. By showing that metabolic flux through the key regulatory enzyme, pyruvate dehydrogenase, is increased in the transition from the fasted to the fed state and is significantly reduced in the diabetic heart, this work represents the first demonstration of the ability of hyperpolarized ^{13}C MRI to non-invasively assess physiological and pathological changes in cardiac metabolism in the human heart. As hyperpolarized ^{13}C MRI allows the *in vivo* visualization of cardiac metabolism, it has major advantages over current non-invasive imaging techniques. Hyperpolarized ^{13}C MRI scans are fast (<2 mins), have no ionizing radiation, and, due to the ability to simultaneously acquire standard MRI acquisitions, have the potential to directly assess perfusion, ischemia, viability, and altered substrate selection in one imaging session.

FIGURE 1

Population Studied

- ○   Type 2 Diabetes (n=13)
  - ○   HbA1c 6-9%, age >18 years
  - ○   No insulin requirement
  - ○   No recent medication change
- ○   Controls (n=12)
  - ○   Age >18 years

Study start @ 7am
Fasting >9 hours

Exclusion Criteria

- ○ Cardiovascular / endocrine / neurological disease
- ○ Hypertension / undiagnosed chest pain
- ○ CKD – eGFR <30 ml/kg/min

Structural / Metabolic Characterization – Fasted State

- ○ Transthoracic Echocardiogram – diastolic function
- ○ CMR CINE Imaging – structural / functional assessment
- ○ ^{1}H Spectroscopy – myocardial steatosis
- ○ ^{31}P MRS – myocardial energetics
- ○ Hyperpolarized [1-^{13}C]Pyruvate MRS – substrate selection
- ○ Laboratory Blood Work

75g oral glucose
(Rapilose®)
45 minutes

Metabolic Characterization – Fed State

- ○ Hyperpolarized [1-^{13}C]Pyruvate MRS – substrate selection
- ○ Total study visit – 2.5 hours

FIGURE 2

Structural Assessment

Metabolic Assessment

Echocardiography   CMR   ³¹P MRS   ¹H MRS   Hyperpolarized ¹³C MRS

PCr

ATP

γ   α   β

Water peak (suppressed)

Lipid peak

[1-¹³C]Lactate

[1-¹³C]Bicarbonate

RV

LV

A

E

FIGURE 3

A Example Spectrum - Fasted Control Subject
Lactate
Alanine
Pyruvate
Bicarbonate

B Example Timecourse - Fasted Control Subject
Pyruvate/20
Bicarbonate
Lactate
CO2
Alanine

C Example Spectrum - Fed Control Subject

D Example Spectrum - Fasted Diabetic Subject

E Example Timecourse - Fasted Diabetic Subject
Pyruvate/20
Bicarbonate
Lactate
CO2
Alanine

F Example Spectrum - Fed Diabetic Subject

FIGURE 4